Macromolecules

Article

pubs.acs.org/Macromolecules

Emulsion Polymerization of Vinyl Acetate in the Presence of Different Hydrophilic Polymers Obtained by RAFT/MADIX

Sandra Binauld, Laura Delafresnaye, Bernadette Charleux, Franck D'Agosto,* and Muriel Lansalot*

Université de Lyon, Université de Lyon 1, CPE Lyon, CNRS, UMR 5265, C2P2 (Chemistry, Catalysis, Polymers & Processes), Team LCPP Bat 308F, 43 Bd du 11 Novembre 1918, 69616 Villeurbanne, France

Supporting Information

ABSTRACT: The surfactant-free emulsion polymerization of vinyl acetate (VAc) was achieved using RAFT/MADIX-mediated polymerization-induced self-assembly (PISA) process in water. First, well-defined hydrophilic macromolecular RAFT agents (macroRAFT) bearing a xanthate chain end were synthesized by RAFT/MADIX polymerization of *N*-vinylpyrrolidone (NVP) and *N*-acryloylmorpholine (NAM) or by post-modification of commercial poly(ethylene glycol). Chain extension of the macroRAFT with VAc in water led to the block copolymer nanoscale organization and the subsequent formation of stable and isodisperse PVAc latex nanoparticles with high solids content (35−37 wt %). The influence of various parameters, including the nature and functionality of the macroRAFT agent precursor, on the polymerization kinetics and particle morphology was also studied.

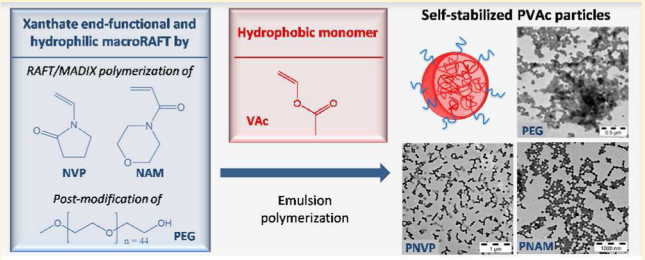

INTRODUCTION

Aqueous emulsion polymerization of vinyl acetate (VAc) is a widely used process that finds industrial applications in various domains such as adhesives, paints, and coatings.[1−3] This process is usually carried out according to a free radical emulsion polymerization of the monomer in water in the presence of surfactant. The developments of the reversible deactivation radical polymerization (RDRP)[4] in water recently allowed to perform emulsion polymerization according to the polymerization-induced self-assembly (PISA) process.[5] PISA is based on the use of a hydrophilic polymer synthesized by RDRP that is extended with hydrophobic monomer units in a monomer-in-water emulsion. The resulting amphiphilic block copolymers can then self-assemble in water[6,7] or simply act as *in situ* formed stabilizers.[8−10] First developed according to a two-pot process consisting in the preparation and the purification of the hydrophilic living precursor and its further use in water, PISA has recently shown to be effective in a one-pot process in which both the syntheses of the hydrophilic precursor and the final particles are performed in water in the same reactor.[11−18] Self-stabilized nano-objects that can further show various morphologies can thus be obtained in a simple synthetic procedure and in the absence of additional molecular surfactant.[15,16,18] Similar concepts have been developed in dispersion polymerization.[5,19] Among the RDRP techniques, reversible addition−fragmentation chain transfer (RAFT) remains the most studied and probably the most versatile one so far. With RAFT, various hydrophobic monomers such as styrenics and (meth)acrylics, or recently vinylidene chloride,[20] have been successfully employed alone or in combination as constitutive monomer units of the hydrophobic core. To control the growth of these hydrophobic blocks and to favor an efficient self-assembly process, the hydrophilic precursor should be synthesized with thiothiocarbonylated chain transfer agents (CTAs) as control agents such as dithioesters or trithiocarbonates. Trithiocarbonates are, however, generally employed since they proved their superiority in controlling the RAFT polymerization of hydrophilic monomer in water and they induce low or even no rate retardation compared to dithiobenzoates. The transposition of the PISA process to the synthesis of PVAc-based particles is thus very challenging but, however, more demanding since the controlled radical polymerization of VAc is not trivial. Indeed, the use of xanthates or dithiocarbonates CTAs in a RAFT process, strategy originally coined as macromolecular design by interchange of xanthates (MADIX),[21] is probably the best way to synthesize well-defined PVAc polymer chains.[22−29] In the frame of the PISA process, this requires the use of hydrophilic macroCTA (macroRAFT) precursors that are carrying dithiocarbonate end groups. These precursors can thus only be obtained either by performing the RAFT/MADIX of a hydrophilic monomer using a dithiocarbonate as control agent or by introducing a dithiocarbonate end group on a preformed hydrophilic polymer chain. As far as we know, only one example reports the VAc emulsion polymerization in water mediated by a preformed dithiocarbonate end-functionalized polymer, namely dextran.[10] The functionalization rate was rather low (ca. 30%) and in this particular system, the

Received: December 13, 2013
Revised: April 29, 2014

   dx.doi.org/10.1021/ma402549x | *Macromolecules* XXXX, XXX, XXX−XXX

formation and the stabilization of the particles were possible by a fraction of *in situ* formed dextran-PVAc block copolymers. Influence of the dextran-CTA and monomer contents on the polymerization was studied, and stable monodisperse PVAc latex particles up to 27 wt % solids content were obtained with fast kinetics for low amounts of dextran-CTA (2−4 wt %). However, the control over the polymerization was not fully efficient as evidenced by the increase of the molar mass dispersity with conversion up to a value of 5.6.

In this paper, a systematic study was thus undertaken to design an efficient PISA system in which the formation of block copolymers would lead to self-assembly and to PVAc polymer particles composed exclusively or not of block copolymers. The first requirement was to identify a hydrophilic macroRAFT agent that could be synthesized using RAFT/MADIX process. The number of hydrosoluble monomers polymerized by RAFT/MADIX and leading to well-defined hydrosoluble polymer is indeed very limited. *N*-Vinylpyrrolidone (NVP) is a hydrosoluble monomer that has been efficiently polymerized in a controlled way using the RAFT/MADIX process.[30] However, the dithiocarbonate chain end of the resulting PNVP macroRAFT is thermally unstable and can be eliminated during polymerization.[31] To prevent these side reactions, Destarac et al. developed recently a robust approach for aqueous RAFT/MADIX polymerization of NVP at ambient temperature using a redox initiation.[32] Poly(acrylamide)-based diblock copolymers were successfully synthesized from PNVP macroRAFT in aqueous solution using the same reaction conditions.

N-Acryloylmorpholine (NAM) is a bisubstituted hydrosoluble acrylamide derivative with interesting features, including the ability to yield polymers that are soluble in water and in a wide range of organic solvents. NAM has been successfully polymerized using the RAFT technique with dithioester or trithiocarbonate chain transfer agents.[33−35] Moreover, PNAM macroRAFTs have been used for the formation of amphiphilic copolymers by chain extension with a variety of hydrophobic monomers.[35−37] Taton et al. only mentioned its polymerization using the RAFT/MADIX process without any experimental data.[38]

Eventually, besides the controlled polymerization of a monomer from a suitable RAFT/MADIX agent, another way of getting a macroRAFT carrying a dithiocarbonate chain end is, as mentioned above, a post-modification of an existing polymer by a xanthate extremity. A common choice for that purpose is to use poly(ethylene glycol) (PEG). Commercially available PEGs prepared via anionic polymerization can be found with one or two hydroxyl end functionalities, which enables a very large range of chemical modifications. Among them, the synthesis of xanthate-functionalized PEG (PEG-X) by post-modification of linear PEG has already been reported in the literature.[39] More specifically, PEG-X has been used for successful xanthate-mediated copolymerization of vinyl acetate in solution.[40−43] To our knowledge, however, no emulsion polymerization of VAc has ever been attempted using this macroRAFT.

In the present paper, we synthesized xanthate-based macroCTAs obtained by RAFT/MADIX polymerization of NVP and by post-modification of linear poly(ethylene glycol) monomethyl ether. In addition, we investigated the RAFT/MADIX of NAM. The use of these hydrophilic precursors in the RAFT/MADIX-mediated emulsion polymerization of vinyl acetate was then studied. Characterization of the final copolymers and latexes was performed using various analytical techniques.

EXPERIMENTAL SECTION

Materials. 4-(Chloromethyl)benzyl alcohol (99%), 2-bromopropionyl bromide (97%), *O*-ethyl xanthic acid potassium salt (96%), *tert*-butyl hydroperoxide Luperox TBH70X (*t*-BuOOH, 70% in water), trioxane, 4,4′-azobis(isobutyronitrile) (AIBN), 4,4′-azobis(4-cyanopentanoic acid) (ACPA), ascorbic acid (Asc Ac), poly(ethylene glycol) methyl ether (PEG, $M_n \approx 2000$ g mol^{-1}, Aldrich), magnesium sulfate were purchased from Aldrich and used as received. *N*-vinylpyrrolidone (NVP, Aldrich, >99%) and vinyl acetate (VAc, Aldrich, analytical standard) were purified by cryodistillation. PEG-X was synthesized as described previously.[40] Xanthates **1** and **2** were synthesized according to existing protocols with minor modifications.[21,41]

Synthesis of the Xanthates. *Synthesis of S-4-(hydroxymethyl)-benzyl carbonodithioate (**1**).* A solution of commercially available *O*-ethyl xanthic acid potassium salt (9.1 g, 56.9 mmol, 1.2 equiv) in ethanol (45 mL) was added dropwise to a solution of 4-(chloromethyl)benzyl alcohol (7.5 g, 47.4 mmol, 1 equiv) in ethanol (35 mL) using a dropping funnel. The mixture was stirred at room temperature for 24 h. The white precipitate of KCl was isolated by filtration, and ethanol was evaporated off. Finally, the product was dissolved in dichloromethane (50 mL) and washed with water (3 × 15 mL). The organic phase was dried over magnesium sulfate and dried under vacuum, yielding a white powder. ^{1}H NMR (ppm, $CDCl_3$), δ: 1.42 (t, 3H, C**H**$_3$), 4.36 (s, 2H, SC**H**$_2$), 4.65 (q, 2H, CH$_3$C**H**$_2$), 4.68 (d, 2H, C**H**$_2$OH), 7.29−7.37 (m, 4H, Ph). ^{13}C NMR (ppm, $CDCl_3$), δ: 13.8 (**C**H$_3$CH$_2$O), 40.1 (C**C**H$_2$S), 65.0 (**C**H$_2$OH), 70.1 (CH$_3$**C**H$_2$O), 127.3 (2**C** *meta*), 129.3 (2**C** *ortho*), 135.2 (**C**CH$_2$S), 140.2 (**C**CH$_2$OH), 213.9 (**C**═SS).

*Synthesis of O-Ethyl S-(1-Phenylethyl) Carbonodithioate (**2**).* A solution of commercially available *O*-ethyl xanthic acid potassium salt (10.4 g, 65 mmol, 1.2 equiv) in ethanol (45 mL) was added dropwise to a solution of 1-bromoethylbenzene (10 g, 54 mmol, 1 equiv) in ethanol (35 mL) using a dropping funnel. The mixture was stirred at room temperature for 24 h. The white precipitate of KBr was isolated by filtration, and ethanol was evaporated off. Finally, the product was dissolved in dichloromethane (50 mL) and washed with water (3 × 15 mL). The organic phase was dried over magnesium sulfate and dried under vacuum, yielding a yellow oil. ^{1}H NMR (ppm, $CDCl_3$), δ: 1.39 (t, 3H, CH$_2$C**H**$_3$), 1.73 (d, 3H, CHC**H**$_3$), 4.62 (tetra, 2H, CH$_3$C**H**$_2$), 4.90 (q, 1H, C**H**CH$_3$), 7.24−7.40 (m, 5H, Ph). ^{13}C NMR (ppm, $CDCl_3$), δ: 13.7 (**C**H$_3$CH$_2$O), 21.7 (SCH**C**H$_3$), 49.2 (S**C**HCH$_3$), 69.7 (CH$_3$**C**H$_2$O), 127.5 (2**C** *ortho*), 128.6 (2**C** *meta*), 141.8 (**C**CHCH$_3$), 213.4 (**C**═SS).

Polymerization of NVP. *Free Radical Polymerization of NVP in Dioxane.* NVP (5 g, 4.5.10^{-2} mol, 1 equiv), AIBN (0.015 g, 9 × 10^{-5} mol, 0.002 equiv), trioxane (0.67 g, 7.5 × 10^{-3} mol, 0.17 equiv), and dioxane (5 mL, 5.86 × 10^{-2} mol) were introduced in a three-neck round-bottom flask. The mixture was degassed by three cycles of freeze−vacuum−thaw then stirred 1 h at 80 °C. The mixture was diluted with CH_2Cl_2 then precipitated twice in diethyl ether and dried under reduced pressure.

Free Radical Polymerization of NVP in Water. NVP (3.44 g, 3.1 × 10^{-2} mol, 1 equiv), *t*-BuOOH (0.054 g, 6.0 × 10^{-4} mol, 0.02 equiv), and trioxane (0.465 g, 5.2 × 10^{-3}, 0.17 equiv) were introduced in a round-bottom flask in 4 mL of deionized water. In a separate flask, ascorbic acid (0.106, 6.0 × 10^{-4} mol, 0.02 equiv) was dissolved in 1 mL of deionized water. The two solutions were degassed under argon for 30 min. The ascorbic acid solution was then added to the mixture under argon, and the polymerization medium was stirred for 48 h at 25 °C. The mixture was freeze-dried and redissolved in ethanol, then precipitated twice in diethyl ether.

RAFT/MADIX Polymerization of NVP in Dioxane. In a typical experiment, NVP (5 g, 4.5 × 10^{-2} mol, 1 equiv), xanthate **1** (0.240 g, 5 × 10^{-3} mol, 0.02 equiv), AIBN (0.015 g, 9 × 10^{-5} mol, 0.002 equiv), trioxane (0.67 g, 7.5 × 10^{-3} mol, 0.17 equiv), and dioxane (5 mL, 5.86 × 10^{-2} mol) were introduced in a three-neck round-bottom flask. The

dx.doi.org/10.1021/ma402549x | *Macromolecules* XXXX, XXX, XXX−XXX

Scheme 1. RAFT/MADIX Polymerization of (a) *N*-Vinylpyrrolidone (NVP) and (b) *N*-Acryloylmorpholine (NAM) Using Xanthates 1 and 2, Respectively

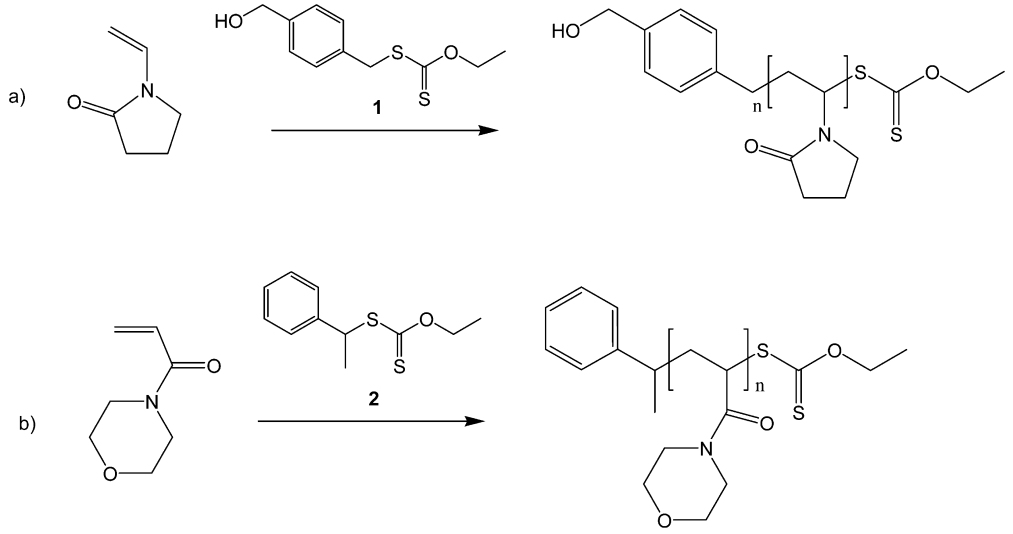

mixture was degassed by three cycles of freeze–vacuum–thaw then stirred 7 h at 80 °C. The mixture was diluted with CH_2Cl_2 then precipitated twice in diethyl ether and dried under reduced pressure.

RAFT/MADIX Polymerization of NVP in Water. In a typical experiment, NVP (3.44 g, 3.1×10^{-2} mol, 1 equiv), xanthate **1** (0.229 g, 9.4×10^{-4} mol, 0.03 equiv), *t*-BuOOH (0.054 g, 6.0×10^{-4} mol, 0.02 equiv), and trioxane (0.465 g, 5.2×10^{-3}, 0.17 equiv) were introduced in a round-bottom flask with 4 mL of deionized water. In a separate flask, ascorbic acid (0.106, 6.0×10^{-4} mol, 0.02 equiv) was dissolved in 1 mL of deionized water. The two solutions were degassed under argon for 30 min. The ascorbic acid solution was then added to the mixture under argon, and the polymerization medium was stirred for 48 h at 25 °C. The mixture was freeze-dried and redissolved in ethanol, then precipitated twice in diethyl ether.

RAFT/MADIX Polymerization of NVP in Bulk. In a typical experiment, NVP (5 g, 4.5×10^{-2} mol, 1 equiv), xanthate **1** (0.240 g, 5×10^{-3} mol, 0.02 equiv) and AIBN (0.015 g, 9×10^{-5} mol, 0.002 equiv) were introduced in a round-bottom flask. The mixture was degassed by three cycles of freeze–vacuum–thaw then stirred 3 h at 80 °C. The mixture was diluted with CH_2Cl_2 then precipitated twice in diethyl ether and dried under reduced pressure.

Polymerization of NAM. *RAFT/MADIX Polymerization of NAM in Dioxane.* In a typical experiment, NAM (2.5 g, 1.8×10^{-2} mol, 1 equiv), xanthate **2** (0.112 g, 5.0×10^{-4} mol, 0.03 equiv), AIBN (0.006 g, 4.0×10^{-5} mol, 0.002 equiv), and trioxane (0.16 g, 1.7×10^{-3}, 0.1 equiv) were introduced in a round-bottom flask with 3.5 mL of dioxane. The solution was degassed under argon for 30 min, then stirred for 5 h at 70 °C. The mixture was precipitated twice in diethyl ether.

RAFT/MADIX Polymerization of NAM in Bulk. In a typical experiment, NAM (1 g, 7.1×10^{-3} mol, 1 equiv), xanthate **2** (0.045 g, 2×10^{-4} mol, 0.03 equiv), and ACPA (0.004 g, 1×10^{-5} mol, 0.002 equiv) were introduced in a round-bottom flask. The solution was degassed under argon for 30 min, then stirred for 1 h at 70 °C. The mixture was diluted with CH_2Cl_2 then precipitated twice in diethyl ether and dried under reduced pressure.

General Procedures for the Emulsion Polymerization of Vinyl Acetate in the Presence of a MacroRAFT (PNVP, PNAM, or PEG). All emulsion polymerizations were performed using the following protocol. VAc, the macroRAFT, and *t*-BuOOH were introduced in a round-bottom flask with deionized water. In a separate flask, ascorbic acid was dissolved in deionized water. The two solutions were degassed under argon for 30 min. The ascorbic acid solution was then added to the mixture under argon, and the polymerization medium was stirred for 48 h at 25 °C. The monomer consumption was followed by gravimetric analysis of samples withdrawn from the polymerization medium at different times. Table 3 displays the experimental conditions of the various RAFT/MADIX VAc emulsion polymerizations and the main features of the resulting PVAc particles.

Analytical Techniques. *Nuclear Magnetic Resonance (NMR).* The overall monomer conversion was determined by ^{1}H NMR spectroscopy of the crude reaction medium diluted with D_2O with a Bruker DRX 300 at room temperature. The chemical shift scale was calibrated relative to the solvent peak and the vinyl protons of the monomers were used to determine the overall conversion using 1,3,5-trioxane protons as an internal reference.

Size Exclusion Chromatography (SEC). Measurements were performed in DMF (+ LiBr, 0.01 mol L^{-1} and toluene as a flow rate marker) at 50 °C at a flow rate of 1.0 mL min^{-1} using a Tosoh EcoSEC HLC-8320GPC equipment (SEC-DMF). All polymers were analyzed at a concentration of 3 mg mL^{-1} after filtration through a 0.45 μm pore-size membrane. The separation was carried out on three PSS GRAM linear columns (300 × 8 mm). The setup was equipped with a refractive index (RI) detector (Waters 410 Differential Refractometer at λ = 930 nm). The average molar masses (number-average molar mass, M_n, and weight-average molar mass, M_w) and the dispersity ($Đ = M_w/M_n$) were derived from the RI signal by a calibration curve based on poly(methyl methacrylate) (PMMA) standards. The software used for data collection and calculation was EmpowerTM Pro version 5.0 from Waters. SEC measurements were also performed in THF at 40 °C at a flow rate of 1 mL min^{-1}, using toluene as a flow rate marker (SEC-THF). They were analyzed at a concentration of 3 mg mL^{-1} after filtration through a 0.45 μm pore-size membrane. The separation was carried out on three columns from Malvern Instruments [T6000 M General Mixed Org (300 × 8 mm)]. The setup (Viscotek TDA305) was equipped with a refractive index (RI) detector (λ = 670 nm). M_n and $Đ$ were derived from the RI signal by a calibration curve based on polystyrene standards (PS from Polymer Laboratories) for the analysis of the block copolymers.

Transmission Electron Microscopy (TEM). Diluted latex samples were dropped on a carbon-Formvar-coated copper grid and dried under air. The samples were examined with a Philips CM120 transmission electron microscope operating at 80 kV (Centre Technologique des Microstructures (CTμ), plateform of the Université Claude Bernard Lyon 1, Villeurbanne, France).

Dynamic Light Scattering (DLS). The intensity-average diameter (D_h) of the latex particles and the dispersity factor (*Poly*) were measured at 25 °C using a Zetasizer Nano Series (Nano ZS) from Malvern Instrument using the Zetasizer 6.2 software. The instrument was calibrated with standard polystyrene latex in water exhibiting a particle size of 220 nm ± 6 nm. Before measurements, the latex

dx.doi.org/10.1021/ma402549x | *Macromolecules* XXXX, XXX, XXX–XXX

Table 1. RAFT/MADIX Polymerization of NVP Controlled by the Xanthate 1, Using Various Conditions

polymer	solvent	init.	[1]/[NVP]	T (°C)	T (h)	f^a (%)	x^b (%)	$M_{n\ th}{}^c$ (g mol^{-1})	$M_{n\ NMR}{}^d$ (g mol^{-1})	$M_{n\ SEC}{}^e$ (g mol^{-1})	$Đ^e$
PNVP1	dioxane	AIBN	0	80	1	–	70	–	–	51190	3.4
PNVP2	dioxane	AIBN	0.022	80	7	55	63	3770	3900	2630	1.3
PNVP3	dioxane	AIBN	0.022	60	24	17	33	1910	2350	1330	1.4
PNVP4	bulk	AIBN	0.022	80	5	51	78	4280	4130	3860	1.3
PNVP5	bulk	AIBN	0.022	80	1.5	86	66	3575	3020	2690	1.3
PNVP6	water	redox	0.022	25	24	55	88	5140	5240	4210	1.6

[a] f is an estimation by ^{1}H NMR of the xanthate functionality in the final macroRAFT. [b] x is the conversion as followed by ^{1}H NMR. [c] Theoretical number-average molar mass, calculated using the experimental conversion x. [d] Molar mass from DP_n estimated by comparing the xanthate chain end to the polymer resonances on the ^{1}H NMR spectra. [e] Values obtained by SEC-DMF according to a conventional calibration against PMMA standards.

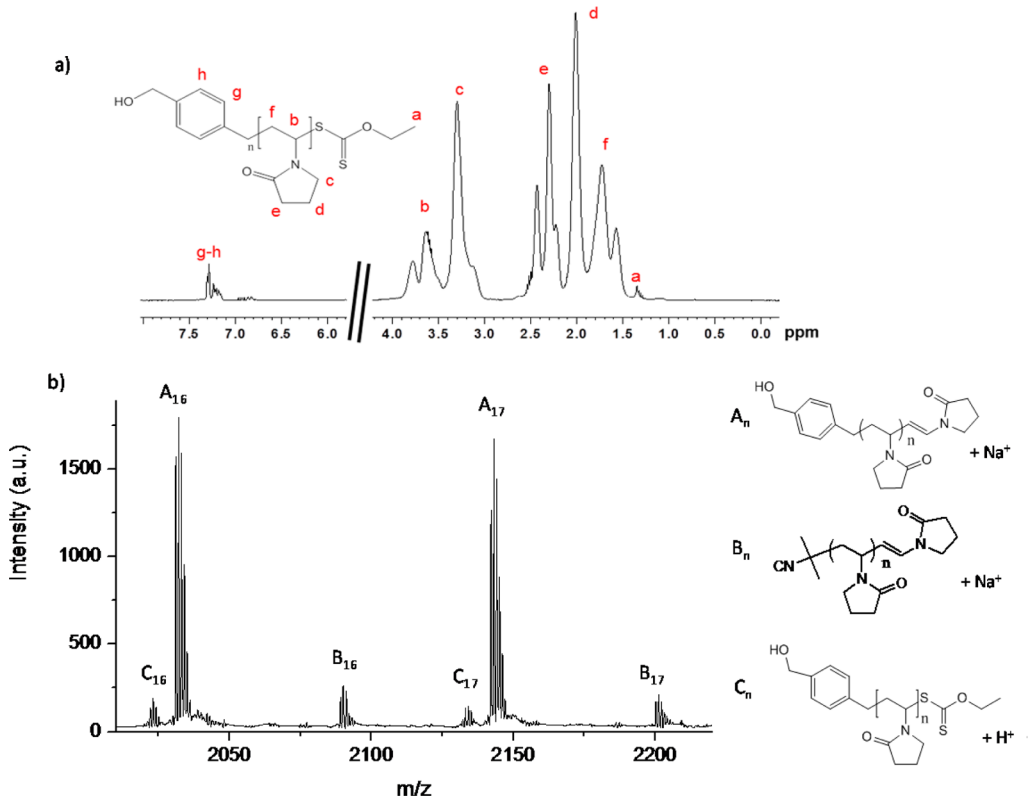

Figure 1. (a) ^{1}H NMR spectrum of **PNVP2** (D_2O). The area between 4.5 and 5.5 ppm is mainly overlapped by the H_2O characteristic resonance and was omitted from the spectrum. (b) Enlarged MALDI–ToF mass spectrum of **PNVP2** in reflectron mode.

samples were diluted in deionized water. The number of particles per liter of the aqueous phase, N_p, was calculated as follows:

$$N_p = \frac{6\tau}{\rho\pi D_h^{\ 3}}$$

with τ (g L$^{-1}{}_{water}$) the solids content of the dispersed phase (τ = ($m_{macroRAFT}$ + conversion × m_{VAc})/V_{water}, with $m_{macroRAFT}$ and m_{VAc} the initial weight of macroRAFT and VAc, respectively, V_{water} the initial volume of water) and ρ the density of PVAc (1.19 g cm^{-3}).

Matrix-Assisted Laser Desorption-Ionization Time-of-Flight Mass Spectrometry (MALDI–ToF–MS). Mass spectra were acquired on a Voyager-DE STR (Applied Biosystems, Framingham, MA). This instrument was equipped with a nitrogen laser (wavelength 337 nm) to desorb and ionize the samples. Samples were analyzed using dithranol as a matrix with or without sodium iodide salt as cationization agent. The accelerating voltage used was 20 kV. The spectra were the sum of 300 shots, and an external mass calibration was used. Samples were prepared by dissolving the product in DMF at a concentration of 1 g L^{-1}. The assigned isotopic distributions were simulated with ISOPRO mass spectrometry simulator before being assigned.

RESULTS AND DISCUSSION

PNVP MacroRAFT Synthesis. The first step of this work was dedicated to the synthesis of PNVP macroRAFT from xanthate-based CTA. *O*-Ethyl *S*-4-(hydroxymethyl)benzyl carbonodithioate (**1**) was chosen to control the polymerization of NVP (Scheme 1a). Polymerization kinetics was studied during the RAFT/MADIX process performed under various conditions of solvent and temperature (Table 1). As a control experiment, the free radical polymerization of NVP was performed in dioxane and yielded high molar mass polymer with broad molar mass distribution (**PNVP1**, Table 1). Then, **1** was used to control the RAFT/MADIX polymerizations of NVP in the same conditions (**PNVP2,** Table 1). The [**1**]/[monomer] ratio was chosen in order to reach molar masses around 5000 g mol^{-1} at 100% conversion.

dx.doi.org/10.1021/ma402549x | *Macromolecules* XXXX, XXX, XXX–XXX

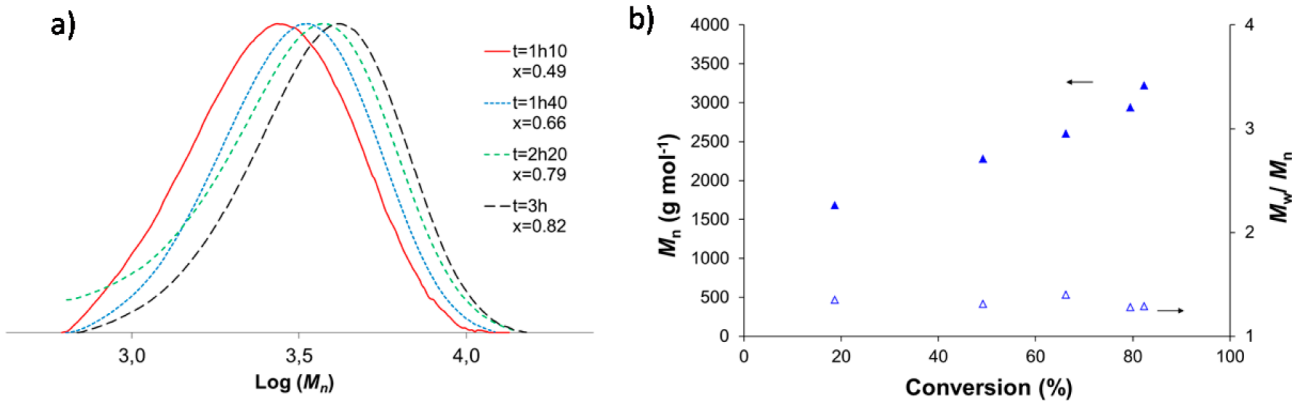

Figure 2. Synthesis of **PNVP5**: (a) SEC-DMF monitoring of the polymerization; (b) Experimental M_n and dispersity as a function of monomer conversion (values obtained from conventional calibration against PMMA standards).

Although that may not be adapted for the determination of absolute molar mass of PNVP, the number-average molar mass (M_n) and the molar mass dispersity values ($Đ$) were estimated by SEC analyses in DMF based on PMMA calibration. **PNVP2** macroRAFT showed much narrower molar mass distribution ($Đ$ = 1.3) compared to the **PNVP1** polymer obtained by free radical polymerization at similar conversions ($Đ$ = 3.4). In addition, as shown in Figure 1a, ^{1}H NMR spectrum of **PNVP2** in deuterium oxide (D_2O) confirmed the formation of polymers carrying an aromatic end group coming from **1**, as expected. Integration of the aromatic protons versus other characteristic polymer peaks allowed an estimation of the macroRAFT molar mass (3900 g mol^{-1}) that was found to be close to the theoretical value (3770 g mol^{-1}, see Table 1). Besides, the presence of a triplet at 1.3 ppm (a) is characteristic of the methyl protons of the ethoxy group carried by the polymer chains and coming from **1**, showing the functionalization of PNVP on the other chain end. This signal is well resolved and can be used to quantify the functionality of PNVP by comparing its integration value to the one of the aromatic protons. Xanthate functionality of **PNVP2** was found to be around 55% according to this technique, suggesting that side reactions occurred under these experimental conditions. In the case of RAFT/MADIX of NVP, the thermal stability of the *O*-ethyl xanthate chain end has been reported to be low, leading to sulfur-free PNVP chains.[44] To complete the characterization, MALDI−ToF−MS analysis was performed on **PNVP2** macroRAFT (Figure 1b). The structure that corresponds to the main population is the $\mathbf{A_n}$ form cationized with sodium and carrying the 4-hydroxymethylbenzyl group on the α chain end coming from **1** and a double bond on the ω end. The absence of xanthate end group is probably due to its fragmentation during the analysis under the MALDI−ToF−MS conditions, as previously discussed by Destarac et al.,[32,45a] and to a fraction of chains that are effectively not carrying a xanthate chain end. Still, the expected population was present although in low proportion ($\mathbf{C_n}$). The presence of the 4-hydroxymethylbenzyl substituent of **1** in these two populations confirmed that **1** efficiently participates in the initiation step. Moreover, this analysis gave access to absolute values of molar mass and dispersity for **PNVP2** (M_n = 3020 g mol^{-1} and $Đ$ = 1.22, see Figure S1 in the Supporting Information for the full distribution), that were in good agreement with values provided by other techniques and with the expected value (M_n = 3770 g mol^{-1}).

To address the PNVP functionality issue, several NVP polymerizations were carried out using different solvent or temperature conditions. As mentioned in the Introduction, the thermal stability of PNVP carrying xanthate end group is low. In a first trial, we decided to conduct the polymerization in dioxane at 60 °C instead of 80 °C (**PNVP3**, Table 1). However, only 23% of conversion was reached after 24 h of reaction, showing a dramatic slow-down of the polymerization. Under these conditions, the formed PNVP underwent a much longer thermal treatment, the functionality dropping to less than 20%. Finally, NVP was polymerized in bulk at 80 °C, using AIBN as initiator (**PNVP4−5**, Table 1). In a first attempt, the reaction was stopped after 5h. High conversion was reached but only 50% functionality was obtained (**PNVP4**). The polymerization was therefore reproduced in the same conditions using a shorter reaction time (1.5 h). Shorter reaction times allowed to prevent the chain end from thermal degradation and to isolate **PNVP5** with the highest functionality (86% according to ^{1}H NMR). Monomer conversion was followed by ^{1}H NMR, showing as expected faster kinetics for the bulk polymerization (Table 1). To further confirm the controlled behavior of the polymerization, SEC-DMF analyses were performed at various conversions. Figure 2 displays the SEC traces obtained for **PNVP5** as an example. It appears that good control was achieved since the SEC trace was completely shifted toward higher molar masses when conversion increased. Moreover, dispersity remained low ($Đ \sim 1.3$) throughout the polymerization in agreement with a successful RAFT/MADIX polymerization process. The values of M_n for PNVP macroRAFTs were generally slightly underestimated compared to the theoretical ones. However, molar mass values obtained by MALDI−ToF−MS analyses of **PNVP5** (M_n = 3200 g mol^{-1} and $Đ$ = 1.21) were once again consistent with the expected value (M_n = 3200 g mol^{-1}). As for macroRAFT **PNVP2**, the structure that corresponds to the main population was the A_n form cationized with sodium and carrying the 4-hydroxymethylbenzyl group on the α chain end coming from **1** and a double bond on the ω end. This chain end, already observed in the case of **PNVP2**, together with the higher functionality determined by ^{1}H NMR for **PNVP5** are consistent with fragmentation during the analysis (see Figure S2 in Supporting Information).

A similar study was recently performed by Destarac et al.[45a] RAFT/MADIX of NVP performed under thermal initiation systematically gave rise to a certain amount of side-products which increased with the polymerization temperature or time.

dx.doi.org/10.1021/ma402549x | *Macromolecules* XXXX, XXX, XXX−XXX

Table 2. RAFT/MADIX Polymerization of NAM Using Various Conditions

polymer	solvent	init.	[2]/[NAM]	T (°C)	T (h)	f^a (%)	x^b (%)	$M_{n\ th}{}^c$ (g mol^{-1})	$M_{n\ RMN}{}^d$ (g mol^{-1})	$M_{n\ SEC}{}^e$ (g mol^{-1})	$Đ$
PNAM1	dioxane	AIBN	0	70	30	–	90	–		16400	6.9
PNAM2	dioxane	AIBN	0.028	70	5	100	86	4580	5730	3500	1.6
PNAM3	bulk	AIBN	0.028	70	0.7	100	70	3460	7140	4230	1.6
PNAM4	water^f	ACPA	0.028	70	1.5	100	90	4780	7140	4600	2.1

$^a f$ is an estimation by ^{1}H NMR of the xanthate functionality in the final macroRAFT. $^b x$ is the conversion as followed by ^{1}H NMR. ^{c} Theoretical number-average molar mass, calculated using the experimental conversion x. ^{d}Molar mass from DP_n estimated by comparing the xanthate chain end to the polymer resonances on the ^{1}H NMR spectra. ^{e}Values obtained by SEC-THF according to a conventional calibration against PS standards. ^{f}10% of dioxane was added to dissolve **2**.

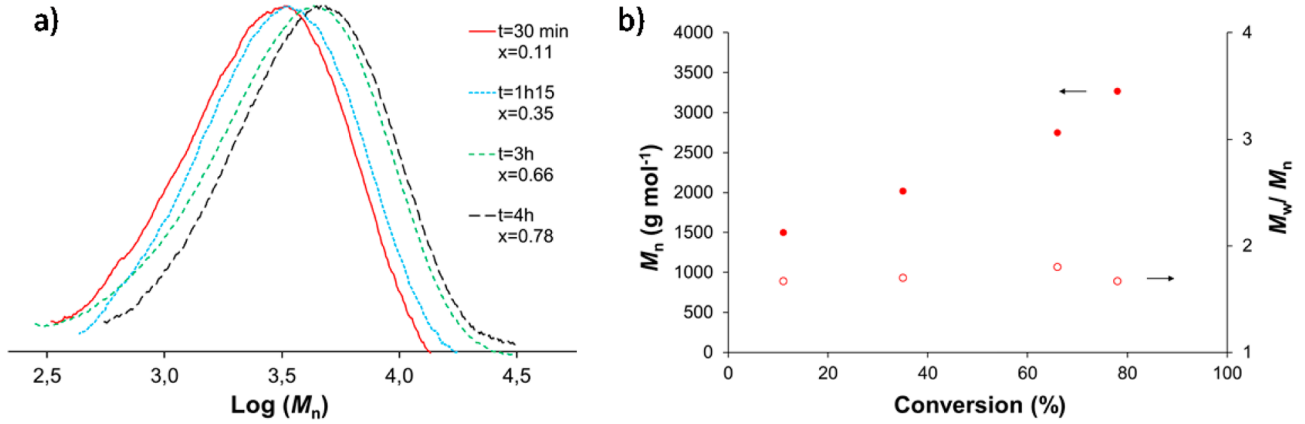

Figure 3. Synthesis of **PNAM2**: (a) SEC-THF monitoring of the polymerization; (b) Experimental M_n and dispersity as a function of monomer conversion (values obtained from conventional calibration against PS standards).

The authors indeed showed and further detailed[32] that when the RAFT/MADIX of NVP was performed in water at 25 °C in the presence of a mixture of *tert*-butyl hydroperoxide and ascorbic acid as initiating system, a very good control of the polymerization was observed and the integrity of xanthate chain ends was kept. In order to investigate the possibility of a one-pot route to block copolymers self-assembly,[11−16] polymerization of NVP was also conducted in water (**PNVP6**, Table 1) under the same conditions. A *tert*-butyl hydroperoxide/ascorbic acid (*t*-BuOOH/Asc Ac) redox initiating system was used at 25 °C to prevent thermal degradation, as previously recommended by Destarac et al.[32] As expected, the polymerization kinetics was much slower, and the polymerization was followed over 24 h to achieve high conversion (88%). ^{1}H NMR analysis revealed that the xanthate functionality was, however, not improved using these conditions (f = 55%), and showed the appearance of hydrolysis degradation products. Destarac et al.[32] reported high fidelity of the xanthate chain end (even after 5 days of storage) when synthesizing PNVP under these conditions. The synthesis of block copolymers using a PNVP macroRAFT was not depicted, although a polyacrylamide-*b*-PNVP could be obtained using a polyacrylamide block obtained by RAFT/MADIX performed in water for the polymerization of NVP. However, we could not reach here the same level of functionality. Therefore, a two-step process employing **PNVP2** or **PNVP5** will be used in the following for the emulsion polymerization of VAc from PNVP macroRAFT. However, during the reviewing process of this manuscript, Destarac et al. reported[45b] the beneficial use of sodium sulfite as reducing agent instead of ascorbic acid for RAFT polymerization of NVP. This system may be of real interest to implement a one-pot process for emulsion polymerization of VAc employing PNVP chains synthesized in water.

PNAM MacroRAFT Synthesis. Since the polymerization of NVP by the RAFT/MADIX process gave macroRAFTs with partial functionality, *N*-acryloylmorpholine (NAM) was chosen as suitable candidate to both achieve potentially highly xanthate functionalized hydrophilic macroRAFT and employ a one-pot approach. As far as we know and as already mentioned in the Introduction, there is no detailed study in the literature on the RAFT/MADIX polymerization of NAM. According to a preliminary study, *O*-ethyl *S*-(1-phenylethyl) carbonodithioate (**2**) was chosen to control the polymerization of NAM (Scheme 1b). As a systematic study, NAM polymerization was also conducted in different media. In a similar way to NVP, free radical polymerization of NAM was performed in dioxane as a control experiment, yielding a polymer with a broad molar mass distribution (M_n = 16 400 g mol^{-1}, $Đ$ = 6.9, **PNAM1**, Table 2). Polymerization was conducted at 70 °C (instead of 80 °C for NVP) to allow conversion monitoring, since the NAM polymerization was proceeding too rapidly at higher temperature. Then, RAFT/MADIX controlled polymerization of NAM was performed in similar conditions using **2** (**PNAM2**, Table 2). The [CTA]/[NAM] ratio was adjusted to target macroRAFTs with molar mass close to 5000 g mol^{-1} at 100% conversion. As for PNVP, SEC analysis of **PNAM2** macroRAFT showed much narrower molar mass distribution ($Đ$ = 1.6) compared to the **PNAM1** polymer obtained by free radical polymerization at similar conversions ($Đ$ = 6.9). The SEC trace was completely shifted toward higher molar masses over time, with M_n values increasing linearly with conversion and dispersities being relatively low and almost constant throughout the polymerization (Figure 3). The dispersity values were in good agreement with a controlled process considering the known moderate reversible chain transfer ability of xanthates for acrylamide monomers in RAFT/MADIX.[38] As for PNVP

dx.doi.org/10.1021/ma402549x | *Macromolecules* XXXX, XXX, XXX−XXX

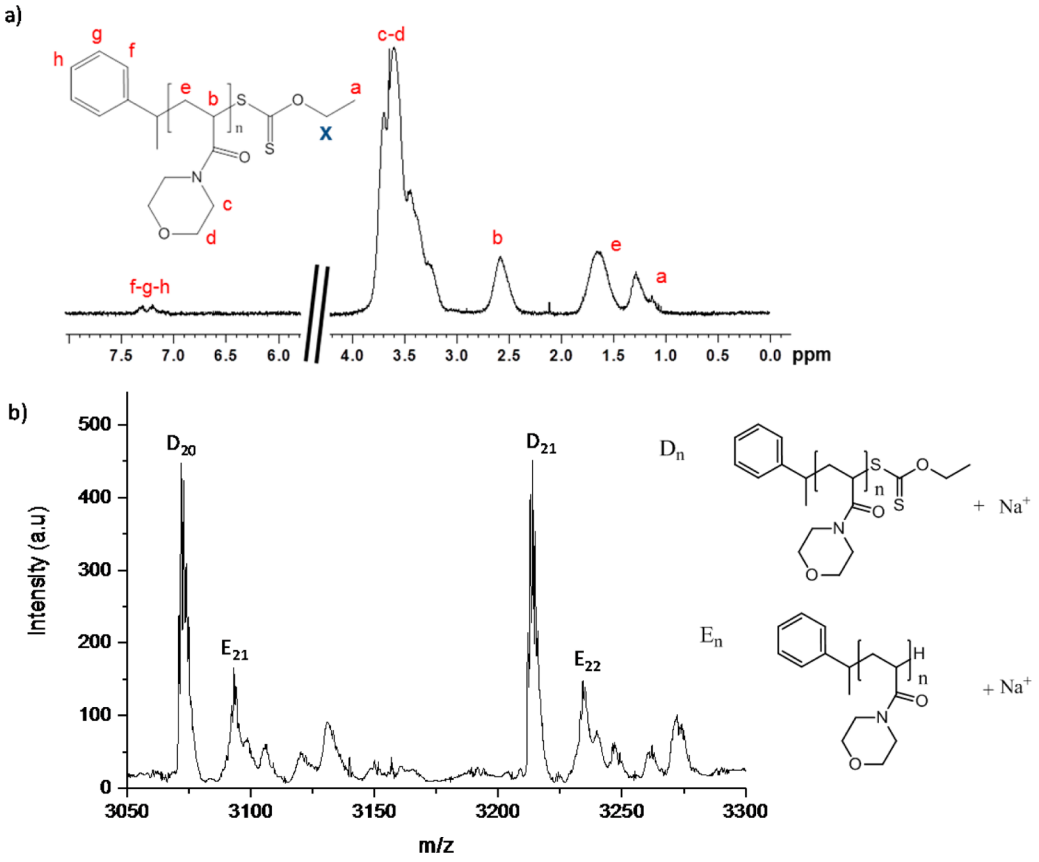

Figure 4. (a) ^{1}H NMR spectrum of **PNAM2** (D_2O). (b) Enlarged MALDI−ToF mass spectrum of **PNAM2** in reflectron mode.

Scheme 2. Synthesis of PEG-X MacroRAFT by Modification of Commercial PEG Methyl Ether

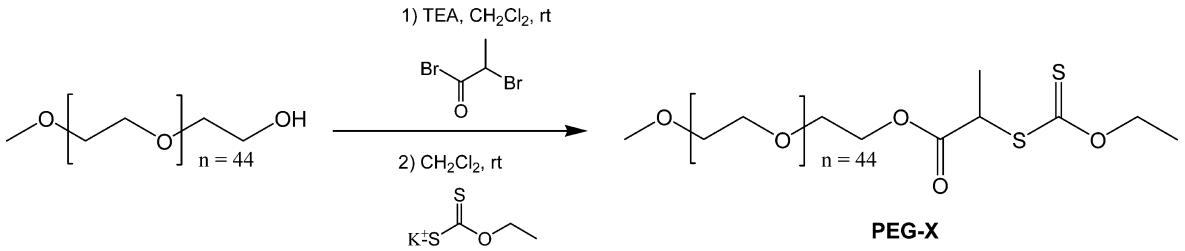

and as already observed for PNAM analyzed by SEC using a conventional calibration based on polystyrene standards,[34] the M_n value of the PNAM macroRAFT was significantly smaller than expected.

^{1}H NMR analysis confirmed the formation of polymer chains carrying an aromatic end group (Figure 4a) coming from **2**. Integration of the aromatic proton signal versus other characteristic polymer resonance (b, 2.6 ppm) allowed an estimation of the macroRAFT molar mass. However, the characteristic signal of the methyl protons of the ethoxy group coming from **2** (a, 1.3 ppm) was overlapped by the broad signal of the methylene protons from the polymer backbone and could not be used to quantify the chain end functionality. ^{1}H NMR analysis of **PNAM2** was therefore also performed in deuterated tetrahydrofuran in which the characteristic signal of the ethoxy group coming from the xanthate signal (**x**, 4.7 ppm in THF-d_8) (see Figure S3 in the Supporting Information) was well resolved. By comparing its integral to the one of the aromatic proton resonance, **PNAM2** was found to be quantitatively functionalized. Also, **PNAM2** was characterized by MALDI−ToF−MS (Figure 4b), revealing that the main population corresponds to the expected structure $\mathbf{D_n}$, cationized with Na^+. The spectrum also shows several populations of lower intensity, probably due to the fragmentation of the xanthate chain ends under the laser beam since no evidence of side products was detected by the other characterization techniques. In a similar way to PNVP macroRAFT, analysis of the MALDI−ToF−MS distribution provided a M_n value (4680 g mol^{-1}, $Đ$ = 1.34) in good agreement with the theoretical value.

Bulk polymerization of NAM was also carried out at 70 °C (**PNAM3**, Table 2), proceeding very quickly since 30% of conversion was reached in a few minutes. The overall conversion was then limited to 70% due to the very high viscosity of the reaction medium. Finally, polymerization was carried out in water using ACPA as initiator (**PNAM4**, Table 2), keeping in mind a one-pot emulsion polymerization process with VAc. Since **2** is not water-soluble, it was preliminarily dissolved in dioxane (10 wt %). However, ^{1}H NMR analysis of the final polymer revealed some traces of unreacted CTA that

dx.doi.org/10.1021/ma402549x | *Macromolecules* XXXX, XXX, XXX−XXX

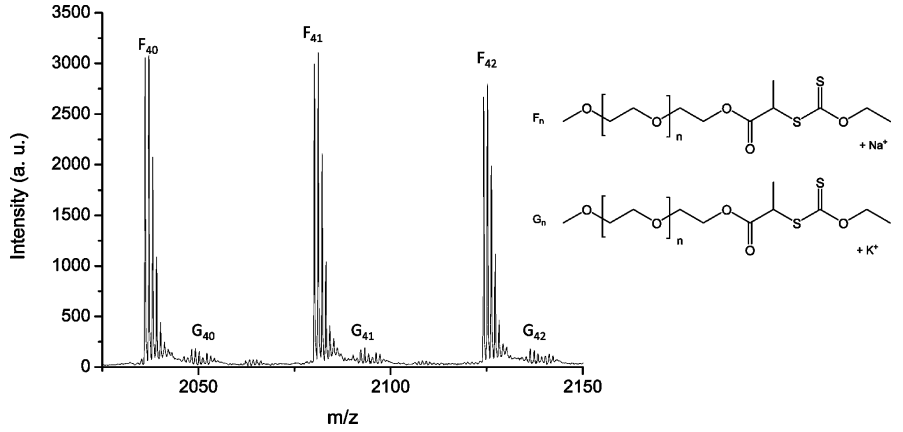

Figure 5. Enlarged MALDI–ToF mass spectrum of **PEG-X** in reflectron mode.

Scheme 3. MADIX Emulsion Polymerization of VAc in Aqueous Medium Using (a) PNVP2 or PNVP5, (b) PEG-X, and (c) PNAM2 MacroRAFTs

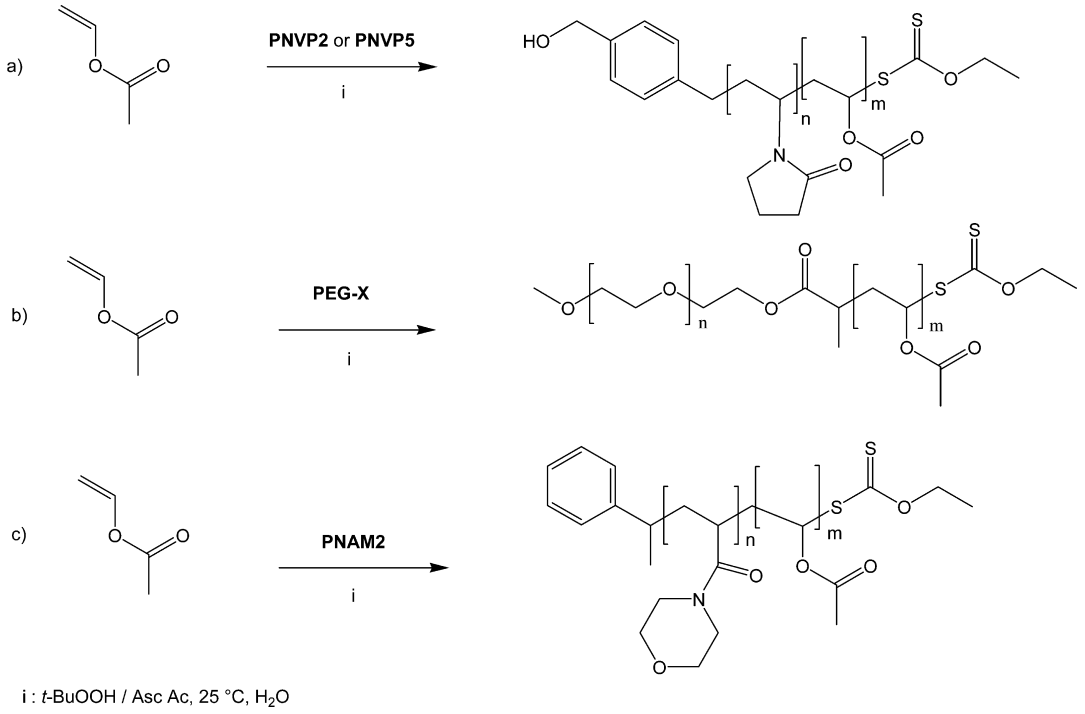

must have precipitated in the polymerization medium. SEC analysis of **PNAM4** showed a broader molar mass distribution ($Đ$ = 2.1) and slightly higher molar mass than expected. Therefore, like in the case of PNVP, the emulsion polymerization of VAc will be performed according to a two-step process using preformed PNAM macroRAFT (**PNAM2**).

PEG-X MacroRAFT Synthesis. A third hydrophilic macroRAFT with a linear structure was synthesized in two steps by modification of commercial poly(ethylene glycol) monomethyl ether of average molar mass M_n = 2000 g mol^{-1} as described previously (Scheme 2).[40] ^{1}H NMR and MALDI–ToF–MS analysis of the macroRAFT confirmed the complete functionalization (Figure 5).

VAc Emulsion Polymerization in the Presence of Xanthate End Functionalized and Hydrophilic Polymers: Synthesis of Self-Stabilized PVAc Latexes. Owing to the poor xanthate functionality of PNVP synthesized in water and the limited control of NAM RAFT/MADIX polymerization in water, the one-pot process was not investigated. Consequently, all the macroRAFT agents used in the surfactant-free RAFT/MADIX VAc emulsion polymerization were those synthesized beforehand in organic solvent, namely **PNVP2**, **PNVP5**, **PNAM2**, and **PEG-X**. As mentioned previously, the xanthate chain end of PNVP macroRAFT is thermally instable and can be eliminated during polymerization. Thus, RAFT/MADIX-mediated emulsion polymerization at ambient temperature using a redox initiation was chosen for this study. The couple *tert*-butyl hydroperoxide/ascorbic acid (*t*-BuOOH/Asc Ac) was used as a redox initiating system (Scheme 3), based on the previous work of Destarac et al.[32] For comparison purposes, the same conditions were applied to the other systems, using PNAM and PEG macroRAFTs, respectively.

Control experiments on emulsion polymerization of VAc were first performed at 25 °C, in absence or presence of xanthate-free **PNVP1** (Table 3, **L0** and **L1**, respectively). In the first case, the polymerization of VAc reached very low

dx.doi.org/10.1021/ma402549x | *Macromolecules* XXXX, XXX, XXX–XXX

Table 3. Aqueous Emulsion Polymerization of VAc in the Presence of PNVP, PNAM, and PEG MacroRAFT Agents

latex[a]	macroRAFT	[CTA] /[VAc]	T (°C)	t (h)	τ_{th}[b] (%)	τ_{exp} (%)	x[c] (%)	$M_{n\ th}$[d] (g mol^{-1})	$M_{n\ SEC}$[e] (g mol^{-1})	$Đ$	D_h[f] (nm)	poly[f]
L0	–	0	25	24	35.5	8.2	16	–	1600	1.5	–	–
L1	**PNVP1**[g]	0.002	25	24	37.5	25.2	55	–	23 020	3.1	380	0.13
L2	**PNVP2**	0.002	25	48	36.9	36.3	89	73 410	25 840	2.2	157	0.02
L3	**PNVP2**	0.004	25	48	37.6	37.4	89	38 590	17 360	2.5	110	0.06
L4	**PNVP2**	0.002	35	5	36.0	35.8	87	71 850	22 660	2.3	268	0.30
L5	**PNVP5**	0.002	25	48	36.1	32.6	75	40 900	18 000	2.3	144	0.11
L6	**PEG-X**	0.002	25	48	35.0	33.9	84	37 970	18 030	2.0	113	0.19
L7	**PNAM2**	0.002	25	48	37.0	33.1	75	37 400	11 000	2.5	140	0.13

[a]For all experiments: 2 mol % of initiator with respect to VAc. [b]Theoretical solid content at 100% conversion. [c]Conversion in VAc monomer calculated by gravimetric analysis. [d]Theoretical M_n calculated from the experimental conversion taking into account the macroRAFT functionality ($M_n = M_{macroRAFT} + M_{VAc}\ (x/[f\ ([CTA]/[VAc])])$). [e]Experimental M_n determined by SEC in THF against PS standards on centrifuged samples. [f]Intensity-average diameter and dispersity factor of the final latex from DLS. [g]PNVP1 was obtained by conventional free-radical polymerization (see Table 1).

conversion and no latex was obtained. In the presence of **PNVP1**, previously obtained by free radical polymerization of NVP, a stable latex was obtained composed of particles with acceptable size dispersity (D_h = 380 nm, poly = 0.13), although SEC analysis of the copolymer revealed a broad molar mass distribution ($Đ$ = 3.1). This result showed that **PNVP1** was involved in the stabilization process. High molar mass PNVP is known to undergo irreversible chain transfer reaction in a free radical process and indeed used as such in dispersion polymerization of hydrophobic monomers to generate in situ grafted amphiphilic polymers able to act as stabilizers.[46,47]

Then, RAFT/MADIX mediated emulsion polymerization of VAc was carried out using macroRAFT **PNVP2** (**L2**, Table 3). This experiment was chosen as reference for the rest of the study. A stable latex was obtained, composed of spheres with a diameter close to 160 nm and rather low size dispersity (Table 3 and Figure 6a). The much lower particle size obtained for **L2** compared to the one obtained when **PNVP1** was used (**L1**, 380 nm) attested to the implication of **PNVP2** through its xanthate chain end in the stabilization of the final objects and thus in the formation of the targeted block copolymers. Indeed, the

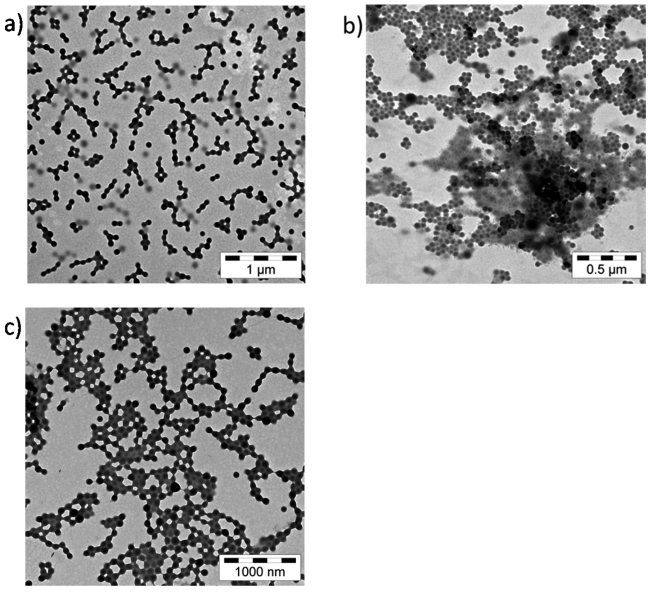

Figure 6. TEM analyses of PVAC latexes: (a) **L2** (from **PNVP2**), (b) **L6** (from **PEG-X**), and (c) **L7** (from **PNAM2**) (see Table 3 for detailed experimental conditions).

comparison of the average number of particles N_p in experiment **L1** and **L2** showed one order of magnitude difference (from 1×10^{16} L^{-1} in **L1** to 2×10^{17} L^{-1} in **L2**). Because of the high water solubility of VAc (2.7×10^{-1} mol L^{-1} at 20 °C),[3] emulsion polymerization of this monomer is usually initiated through homogeneous nucleation, which is probably the case in **L1**. When adding **PNVP2**, a competition between homogeneous nucleation and nucleation by self-assembly of the forming block PNVP-*b*-PVAc copolymers will take place leading to the formation of a higher number of particles. This first observation is a good indication of the enrollment of the xanthate chain end in the stabilization process. SEC analyses of the dry extract of the crude latex indicated the presence of a broad molar mass distribution, probably corresponding to the formed copolymers, as well as residual unfunctionalized **PNVP2** macroRAFT chains (Figure 7a). The two populations were successfully separated by centrifugation of the latex and characterized by ^{1}H NMR, SEC and gravimetric analysis. Analysis of the supernatant after drying confirmed the presence of unreacted **PNVP2**, the amount of which was estimated to be around 40 wt % by gravimetric analysis of the initial amount of **PNVP2**. This percentage was in good agreement with the 55% of functionality observed by NMR for macroRAFT **PNVP2**, and should lead to a maximum of 55% of **PNVP2** chains elongated with VAc. These results also indicate that the stabilization of **L2** is essentially ensured by the extension of xanthate-functionalized chains in **PNVP2** via the RAFT/MADIX process, rather than by irreversible transfer reactions underwent by unfunctionalized PNVP (as observed for **L1**). The SEC analysis of the particles purified by centrifugation gave the copolymer molar mass distribution (M_n = 25 840 g mol^{-1}, $Đ$ = 2.2). Although the dispersity remained high, the shift in molar mass observed was consistent with an elongation of **PNVP2** chains with VAc units. M_n value was obtained by conventional calibration based on polystyrene standards and was not representative of the copolymer molar mass. As for PNVP chains were eliminated in the supernatant, the presence of NVP units in the ^{1}H NMR spectrum of the centrifuged latex confirmed the formation of a block copolymer (see Figure S4 in the Supporting Information). As **PNVP2** was not fully functionalized, higher copolymer molar mass was expected (73410 g mol^{-1}) compared to the theoretical value based on a fully functional PNVP, meaning that the M_n obtained by SEC was probably underestimated compared to the actual copolymer molar mass.

dx.doi.org/10.1021/ma402549x | *Macromolecules* XXXX, XXX, XXX−XXX

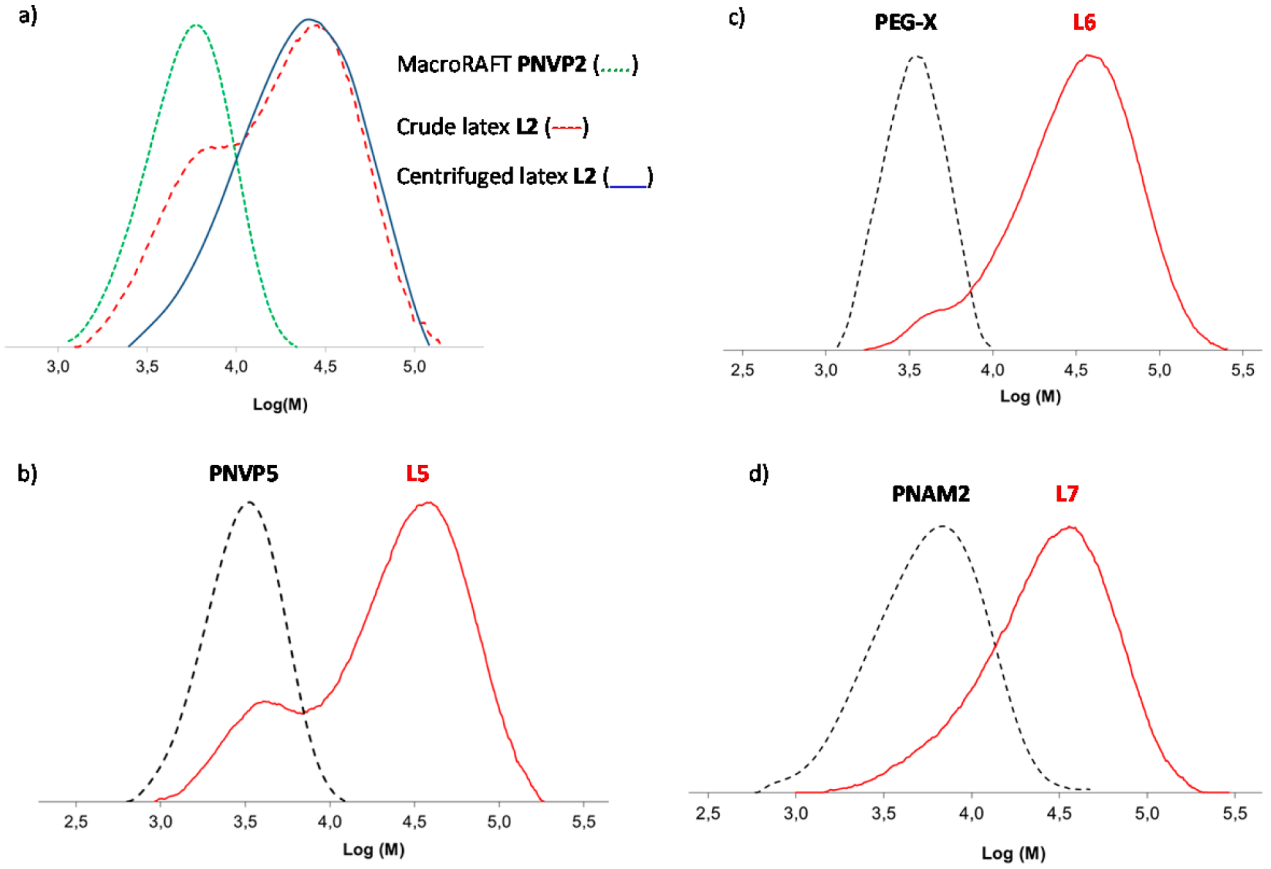

Figure 7. SEC traces in DMF of (a) **PNVP2**, crude latex **L2**, **L2** after centrifugation, (b) **PNVP5** MacroRAFT and crude latex **L5**, (c) **PEG-X** MacroRAFT and crude latex **L6**, and (d) **PNAM2** macroRAFT and crude latex **L7**.

RAFT/MADIX mediated emulsion polymerizations of VAc were then carried out from the macroRAFT **PNVP2** using a two-fold concentration of macroCTA for the same VAc amount (**L3**, Table 3), to target a lower degree of polymerization of the PVAc block. A stable latex composed of spherical particles was obtained as confirmed by DLS (Table 3). Compared to latex **L2**, and for similar conversion (89%), the molar mass of the copolymer as well as the particle diameter were smaller. These results both corroborate the *in situ* formation of block copolymers acting as efficient stabilizers of the PVAc particles. But, again, the molar mass distribution was quite broad ($Đ$ = 2.5). This can likely be related to irreversible transfer reactions,[48] both VAc and PVAc being prone to hydrogen abstraction by radical species ($C_{tr,VAc} \approx 1.77-2.8 \times 10^{-4}$ and $C_{tr,\ PVAc} \approx 1-5 \times 10^{-4}$).[3]

In the next experiment, the temperature was increased to 35 °C to increase the polymerization rate (**L4**, Table 3). High conversion (87%) was obtained after only 5 h of reaction (instead of 48h in the previous cases). Despite a faster polymerization, this latex showed larger particles (D_h = 268 nm) with broader dispersity (poly = 0.3). Complementary ^{1}H NMR analyses proved that PNVP chains were degraded by both hydrolysis and thermolysis. These chains were not available for chain extension and less block copolymers were thus produced resulting in the formation of bigger particles. Finally, emulsion polymerization of VAc was attempted using a PNVP macroCTA of higher xanthate functionality, i.e. **PNVP5** (**L5**, Table 3). SEC trace of the crude latex shows evidence of unreacted PNVP although this population seems to be smaller than in latex **L2** (Figure 7b). Indeed, the analysis of the supernatant after drying confirmed the presence of unreacted PNVP5, the amount of which was estimated to be around 20 wt % of the initial amount of **PNVP5**. As expected, the presence of a higher amount of xanthate functionalized PNVP chains led to the formation of lower molar mass block copolymers (M_n = 18 000 g mol^{-1} for **L5** versus 25 840 g mol^{-1} for **L2**) and to lower particle size (D_h = 144 nm for **L5** versus 157 nm for **L2**).

To overcome the PNVP chain end degradation issue, fully functional macroCTAs **PEG-X** and **PNAM2** were used in a second time to mediate another set of polymerizations of VAc in similar conditions (Table 3, **L6**–**L7**, respectively). Kinetics of VAc polymerization was followed over 48 h by ^{1}H NMR, SEC and gravimetric analysis for the three latexes **L5** (macroRAFT **PNVP5**), **L6** (macroRAFT **PEG-X**), and **L7** (macroRAFT **PNAM2**). Figure 8a shows the evolution of monomer conversion with time for these three experiments during the emulsion polymerization step. For the three experiments, an induction period was observed corresponding to time required for the first VAc units to add onto the macroRAFT and to form an amphiphilic block copolymer. At the onset of block copolymers self-assembly, the polymerization started. An induction period of 2 h was observed for the polymerization of VAc using **PNAM2** macroRAFT (**L7**), whereas this period was longer for polymerizations **L5** and **L6**, based on **PEG-X** and **PNVP5** macroRAFTs, respectively. **L5** and **L6** exhibited slower kinetics with less than 40% of conversion after 16 h of polymerization while **L7** reached ca. 60%.

TEM analyses of the corresponding latexes indicated the formation of particles of controlled size, with a slightly smaller

dx.doi.org/10.1021/ma402549x | *Macromolecules* XXXX, XXX, XXX–XXX

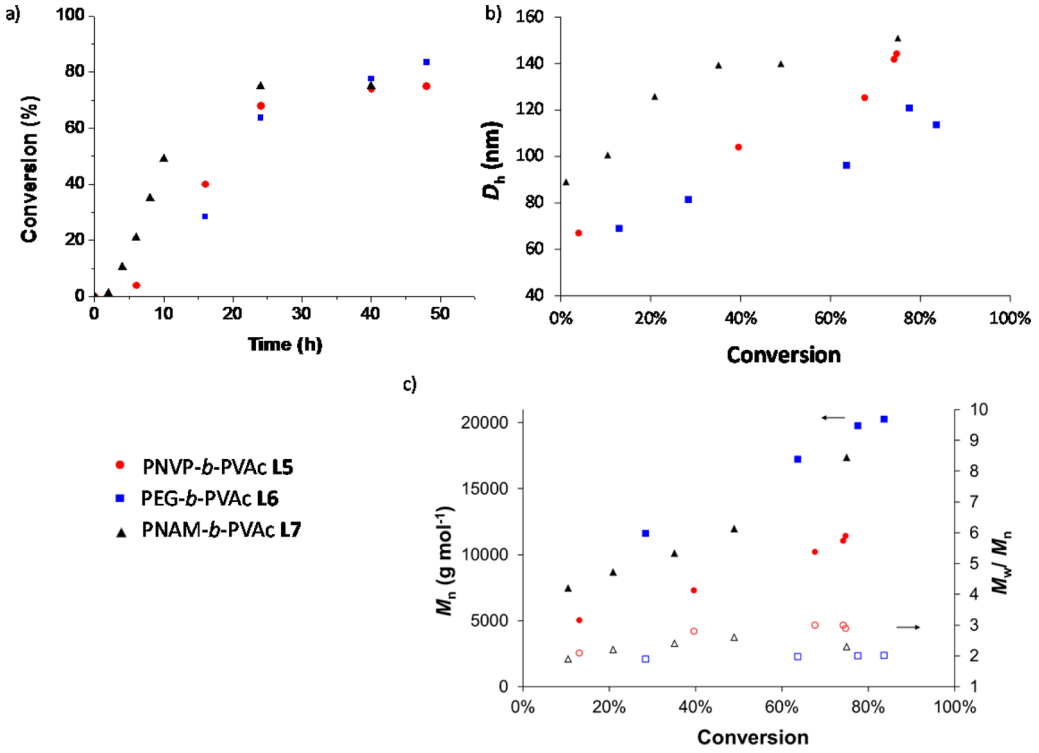

Figure 8. Kinetic study of the synthesis of latexes **L5** (PNVP5), **L6** (PEG-X), and **L7** (PNAM2) via aqueous RAFT/MADIX-mediated emulsion polymerization. (a) Evolution of the conversion of VAc with time. (b) Evolution of the particles diameter versus VAc conversion followed by DLS. (c) Evolution of the number-average molar mass (M_n, full symbols) and dispersity values (M_w/M_n, open symbols) with monomer conversion (values obtained by conventional calibration against PS standards).

diameter in the case of latex **L6** (**PEG-X**) (Figure 6b and 6c). The evolution of the particle size with conversion was followed by DLS analysis for latexes **L5**, **L6**, and **L7** (Figure 8b). The same trend was observed for all latexes, showing the formation of nanoparticles in a range of 60−80 nm at low conversion, increasing gradually in diameter until complete conversion was reached. The final particles diameter was also found to be stable over several weeks, as shown by complementary analyses.

The number-average molar masses increased linearly with VAc conversion, consistent with controlled polymerizations (Figure 8c). The molar mass values could, however, not be compared from one experiment to the other due to the different chemical nature of the hydrophilic segment of the considered block copolymers. The chromatograms of the crude final latexes revealed traces of a secondary distribution for sample **L6** that may be due to a partial degradation of the **PEG-X** during the polymerization process, since no evidence of side products was observed on the purified macroRAFT (Figure 7c). One single distribution was observed for PNAM-based copolymer from latex **L7**, although a small tailing on the low mass side could be observed resulting in a molar mass dispersity that was slightly higher than for the other copolymers (Figure 7d).

CONCLUSIONS

Three different xanthate-terminated hydrophilic polymers were synthesized to serve as macroRAFT precursors in RAFT/MADIX-mediated emulsion polymerization of vinyl acetate. First, poly(*N*-vinylpyrrolidone) and poly(*N*-acryloylmorpholine) were obtained in a controlled way by RAFT/MADIX polymerization of the corresponding monomers. Influence of several parameters on the kinetics of polymerization and functionality of the macroRAFTs were thoroughly investigated. A poly(ethylene glycol)-based macroRAFT was also synthesized by post-modification of a commercial polymer. These hydrophilic precursors were then involved in the surfactant-free RAFT/MADIX-mediated emulsion polymerization of vinyl acetate using a redox initiating system. The self-assembly process induced by the VAc polymerization led to spherical nano-objects that displayed narrow size dispersity and diameters in a 100−200 nm range. PNVP and PEG mediated emulsion polymerizations exhibited slow kinetics and the presence of dead chains of macroRAFT, whereas PNAM mediated one showed faster kinetics and no trace of degradation product, in the same conditions. Thermal RAFT/MADIX-mediated emulsion polymerization of VAc (or its copolymerization with other nonactivated monomers) using the same macroCTAs may lead to faster kinetics and new particles morphologies. These researches are currently under investigation in our laboratories.

ASSOCIATED CONTENT

Supporting Information

MALDI−ToF mass spectra and ^{1}H NMR spectra. This material is available free of charge via the Internet at http://pubs.acs.org.

AUTHOR INFORMATION

Corresponding Authors

*(F.D.) franck.dagosto@univ-lyon1.fr.
*(M.L.) muriel.lansalot@univ-lyon1.fr.

Notes

The authors declare no competing financial interest.

dx.doi.org/10.1021/ma402549x | *Macromolecules* XXXX, XXX, XXX−XXX

■ ACKNOWLEDGMENTS

The authors would like to thank Emilie Grossi (C2P2) and Malvern Instruments SA for technical support. B.C. thanks the Institut Universitaire de France for her nomination as senior member.

■ REFERENCES

(1) Cresswell, M. A.; Holland, K. *Preservation of aqueous-based synthetic polymer emulsions and adhesive formulations In Preservation of Surfactant Formulations*; Morpeth, F. F., Ed.; Springer: Berlin, 1995; p 212−261.
(2) Krieger, S.; Gohr, K.; Fichtner, T.; Rumrich, S. *Eur. Coat. J.* **2010**, 20−23.
(3) Erbil, H. Y. *Vinyl Acetate Emulsion Polymerization and Copolymerization with Acrylic Monomers*; CRC Press: Boca Raton, FL, 2000.
(4) Jenkins, A. D.; Jones, R. G.; Moad, G. *Pure Appl. Chem.* **2010**, *82*, 483−491.
(5) Charleux, B.; Delaittre, G.; Rieger, J.; D'Agosto, F. *Macromolecules* **2012**, *45*, 6753−6765.
(6) Boissé, S.; Rieger, J.; Belal, K.; Di-Cicco, A.; Beaunier, P.; Li, M.-H.; Charleux, B. *Chem. Commun.* **2010**, *46*, 1950−1952.
(7) Zhang, X.; Boissé, S.; Zhang, W.; Beaunier, P.; D'Agosto, F.; Rieger, J.; Charleux, B. *Macromolecules* **2011**, *44*, 4149−4158.
(8) Manguian, M.; Save, M.; Charleux, B. *Macromol. Rapid Commun.* **2006**, *27*, 399−404.
(9) dos Santos, A. M.; Pohn, J.; Lansalot, M.; D'Agosto, F. *Macromol. Rapid Commun.* **2007**, *28*, 1325−1332.
(10) Bernard, J.; Save, M.; Arathoon, B.; Charleux, B. *J. Polym. Sci., Part A: Polym. Chem.* **2008**, *46*, 2845−2857.
(11) Chaduc, I.; Zhang, W.; Rieger, J.; Lansalot, M.; D'Agosto, F.; Charleux, B. *Macromol. Rapid Commun.* **2011**, *32*, 1270−1276.
(12) Chaduc, I.; Girod, M.; Antoine, R.; Charleux, B.; D'Agosto, F.; Lansalot, M. *Macromolecules* **2012**, *45*, 5881−5893.
(13) Chaduc, I.; Crepet, A.; Boyron, O.; Charleux, B.; D'Agosto, F.; Lansalot, M. *Macromolecules* **2013**, *46*, 6013−6023.
(14) Zhang, W.; D'Agosto, F.; Boyron, O.; Rieger, J.; Charleux, B. *Macromolecules* **2011**, *44*, 7584−7593.
(15) Zhang, W.; D'Agosto, F.; Boyron, O.; Rieger, J.; Charleux, B. *Macromolecules* **2012**, *45*, 4075−4084.
(16) Zhang, W.; D'Agosto, F.; Dugas, P.-Y.; Rieger, J.; Charleux, B. *Polymer* **2013**, *54*, 2011−2019.
(17) Brusseau, S.; D'Agosto, F.; Magnet, S.; Couvreur, L.; Chamignon, C.; Charleux, B. *Macromolecules* **2011**, *44*, 5590−5598.
(18) Groison, E.; Brusseau, S.; D'Agosto, F.; Magnet, S.; Inoubli, R.; Couvreur, L.; Charleux, B. *ACS Macro Lett.* **2012**, *1*, 47−51.
(19) Sun, J.-T.; Hong, C.-Y.; Pan, C.-Y. *Polym. Chem.* **2013**, *4*, 873−881.
(20) Velasquez, E.; Rieger, J.; Stoffelbach, F.; Charleux, B.; D'Agosto, F.; Lansalot, M.; Dufils, P.-E.; Vinas, J. *Polymer* **2013**, *54*, 6547−6554.
(21) Destarac, M.; Bzducha, W.; Taton, D.; Gauthier-Gillaizeau, I.; Zard, S. Z. *Macromol. Rapid Commun.* **2002**, *23*, 1049−1054.
(22) Dufils, P. E.; David, G.; Boutevin, B.; Woodward, G.; Otter, G.; Guinaudeau, A.; Mazieres, S.; Destarac, M. *J. Polym. Sci., Part A: Polym. Chem.* **2012**, *50*, 1997−2007.
(23) Fleet, R.; McLeary, J. B.; Grumel, V.; Weber, W. G.; Matahwa, H.; Sanderson, R. D. *Macromol. Symp.* **2007**, *255*, 8−19.
(24) Lou, Y.; Shi, D.; Dong, W.; Chen, M. *Adv. Mater. Res.* **2013**, *645* (10−14), 16.
(25) Nguyen, D. H.; Wood, M. R.; Zhao, Y.; Perrier, S.; Vana, P. *Macromolecules* **2008**, *41*, 7071−7078.
(26) Ozguc, C.; Helvacioglu, E.; Nugay, N.; Nugay, T. *Macromol. Symp.* **2013**, *323*, 18−25.
(27) Simms, R. W.; Davis, T. P.; Cunningham, M. F. *Macromol. Rapid Commun.* **2005**, *26*, 592−596.
(28) Stenzel, M. H.; Cummins, L.; Roberts, G. E.; Davis, T. P.; Vana, P.; Barner-Kowollik, C. *Macromol. Chem. Phys.* **2003**, *204*, 1160−1168.
(29) Zhang, S.; Chen, K.; Liang, L.; Tan, B. *Polymer* **2013**, *54*, 5303−5309.
(30) Wan, D.; Satoh, K.; Kamigaito, M.; Okamoto, Y. *Macromolecules* **2005**, *38*, 10397−10405.
(31) Pound, G.; Eksteen, Z.; Pfukwa, R.; McKenzie, J. M.; Lange, R. F. M.; Klumperman, B. *J. Polym. Sci., Part A: Polym. Chem.* **2008**, *46*, 6575−6593.
(32) Guinaudeau, A.; Mazières, S.; Wilson, D. J.; Destarac, M. *Polym. Chem.* **2012**, *3*, 81−84.
(33) Favier, A.; Charreyre, M.-T.; Chaumont, P.; Pichot, C. *Macromolecules* **2002**, *35*, 8271−8280.
(34) D'Agosto, F.; Hughes, R.; Charreyre, M.-T. r. s.; Pichot, C.; Gilbert, R. G. *Macromolecules* **2003**, *36*, 621−629.
(35) Albertin, L.; Wolnik, A.; Ghadban, A.; Dubreuil, F. *Macromol. Chem. Phys.* **2012**, *213*, 1768−1782.
(36) de Lambert, B.; Charreyre, M.-T.; Chaix, C.; Pichot, C. *Polymer* **2007**, *48*, 437−447.
(37) Jo, Y. S.; van der Vlies, A. J.; Gantz, J.; Antonijevic, S.; Demurtas, D.; Velluto, D.; Hubbell, J. A. *Macromolecules* **2008**, *41*, 1140−1150.
(38) Taton, D.; Destarac, M.; Zard, S. Z. *Macromolecular Design by Interchange of Xanthates: Background, Design, Scope and Applications In Handbook of RAFT Polymerization*; Wiley-VCH Verlag GmbH & Co. KGaA: Weinheim, Germany, 2008; p 373−421.
(39) Shi, L.; Chapman, T. M.; Beckman, E. J. *Macromolecules* **2003**, *36*, 2563−2567.
(40) Lipscomb, C. E.; Mahanthappa, M. K. *Macromolecules* **2011**, *44*, 4401−4409.
(41) Pound, G.; Aguesse, F.; McLeary, J. B.; Lange, R. F. M.; Klumperman, B. *Macromolecules* **2007**, *40*, 8861−8871.
(42) Chen, K.; Grant, N.; Liang, L.; Zhang, H.; Tan, B. *Macromolecules* **2010**, *43*, 9355−9364.
(43) Tong, Y.-Y.; Dong, Y.-Q.; Du, F.-S.; Li, Z.-C. *J. Polym. Sci., Part A: Polym. Chem.* **2009**, *47*, 1901−1910.
(44) Pound, G.; McKenzie, J. M.; Lange, R. F. M.; Klumperman, B. *Chem. Commun.* **2008**, *0*, 3193−3195.
(45) (a) Destarac, M.; Blidi, I.; Coutelier, O.; Guinaudeau, A.; Mazières, S.; Van Gramberen, E.; Wilson, D. J. *Aqueous RAFT/MADIX Polymerization: Same Monomers, New Polymers? In Progress in Controlled Radical Polymerization: Mechanisms and Techniques*; Serie, A. S., Ed.; Wiley: New York, 2012; Vol. *1100*, p 259. (b) Guinaudeau, A.; Coutelier, O.; Sandeau, A.; Mazières, S.; Nguyen Thi, H. D.; Le Drogo, V.; Wilson, D. J.; Destarac, M. *Macromolecules* **2014**, *47*, 41−50.
(46) Vanderhoff, J. W.; Sheu, H. R.; El-Aasser, M. S. *NATO ASI Ser., Ser. C* **1990**, *303*, 529−565.
(47) Fujii, S.; Iddon, P. D.; Ryan, A. J.; Armes, S. P. *Langmuir* **2006**, *22*, 7512−7520.